Eur. Phys. J. D **23**, 189–199 (2003)
DOI: 10.1140/epjd/e2003-00031-y

THE EUROPEAN PHYSICAL JOURNAL D

Sodium in a strong magnetic field

R. González-Férez[a] and P. Schmelcher

Theoretische Chemie, Physikalisch-Chemisches Institut, Im Neuenheimer Feld 229, 69120 Heidelberg, Germany

Received 5 November 2002
Published online 4 February 2003

Abstract. We investigate the effects of a magnetic field with low to intermediate strength on several spectroscopic properties of the sodium atom. A model potential is used to describe the core of sodium, reducing the study of the system to an effective one-particle problem. All states with principal quantum numbers $n = 3, 4, 5, 6$ and 7 are studied and analysed. A grid of twenty values for the field strength in the complete regime $B = 0 - 0.02$ a.u. is employed. Ionisation energies, transition wavelengths and their dipole oscillator strengths are presented.

PACS. 32.30.-r Atomic spectra – 32.70.Cs Oscillator strengths, lifetimes, transition moments – 32.60.+i Zeeman and Stark effects

1 Introduction

The behaviour and the properties of matter in an intense magnetic field is a subject of major interest in physics. Systems exposed to magnetic fields represent active research subjects in disciplines as different as astrophysics, condensed matter physics or atomic physics. On a fundamental level the competing magnetic and interaction forces yield nonintegrable complex systems which can be described theoretically only by developing and applying corresponding nonperturbative methods. The discovery of strong magnetic fields in certain compact astrophysical objects was an important stimulus for the study of atoms and molecules in strong fields. In particular, magnetic white dwarf stars and neutron stars (with field strengths of $B \sim 10^2$–10^5 T and $B \sim 10^7$–10^9 T, respectively), provide "cosmic laboratories" to observe atomic systems under extreme conditions that are not available terrestrially.

In the case of the hydrogen atom the presence of the magnetic field destroys the spherical symmetry of the system. Due to the mixture of the symmetries of both forces the problem becomes non-separable and the atomic structure is changed drastically with increasing field strength. A large variety of structural as well as dynamical phenomena are therefore obtained. For weak field strengths, *i.e.* in the low field regime, the magnetic field can be considered as a perturbation compared to the Coulomb interaction. The approximate spherical symmetry dominates the system and the problem can be solved using perturbation theoretical techniques. In the limit of very strong magnetic fields, the cylindrical symmetry of the interaction with the external field dominates the problem. In this high field regime the adiabatic approximation has been applied to describe the system, although this approximation is strictly valid only in the extreme limit $B \to \infty$. The problem is particularly complicated for the intermediate field regime, where the Lorentz force acting on the atomic electrons equals or exceeds the Coulomb binding force. In such a case non-perturbative numerical methods become necessary. The absolute values of the field strength belonging to the intermediate regime depends on the electronic degree of excitation of the atom: for Rydberg states of atoms laboratory field strengths suffice to enter this regime. We remark that increasingly stronger fields become available in the laboratory: static fields up to 40 T and pulsed fields of ms duration up to several hundred tesla are available in a new generation of laboratories.

Most of the works in the literature have been dealing with the hydrogen atom in a magnetic field for field strengths ranging from the low field to the high field regime. Special efforts were undertaken to address the intermediate regime for which a large number of numerical methods were invented to solve the associated Schrödinger equation [1–6]. However only a few of them provided us with highly accurate spectroscopies data (see Ref. [6] and references therein but more recently also [7]). With the help of these data several observed absorption spectra of magnetic white dwarf stars could be explained, and a simulation of their atmospheres was accomplished. (See Ref. [6] for a comprehensive review in atoms in strong magnetic field and their astrophysical applications until 1994, for a more recent review of atoms and molecules in external fields see [8] and for recent applications to magnetic white dwarfs see Ref. [9].) Only a few of the developed methods were efficient and accurate enough to describe highly excited Rydberg states of hydrogen in magnetic fields.

[a] e-mail: rosario@tc.pci.uni-heidelberg.de

In recent years an extensive and precise study of the helium atom in a external magnetic field became possible [10–13]. To achieve this a new methodological and computational scheme had to be invented and implemented. A significant number of excited states with different symmetries were studied for a broad range of magnetic field strengths. The analysis of the structure of helium in a magnetic field is much more complicated because the electron-electron interaction has to be taken into account. The large amount of data, that have finally been provided, allowed to interpret the spectrum of the prominent white dwarf GD229 [14], that was unexplained for almost 25 years. Furthermore, these results were used to explain spectra of magnetic white dwarf stars which one could not identify to possess magnetized hydrogen [9]. For a review in magnetic white dwarf stars see references [9,15].

Although the atomic structure of hydrogen and helium in a magnetic field have allowed for the interpretation of absorption features of several magnetic white dwarfs, there are other magnetic objects whose spectra can not been explained in terms of these two atomic systems. In addition, due to the increasing availability of observatories with higher resolutions and sensitivities, new spectra have been obtained that could not be explained [16], thereby opening the necessity for studies of heavier atoms exposed to magnetic fields. In particular, there are some observations of magnetic white dwarfs of type DZ, which features can be explained in terms of atomic data of elements like Na, Mg, Ca and even Fe [17]. It is believed that these heavy atoms are present in the atmospheres of the corresponding stars due to accretion of interstellar matter, and particularly it is expected that these objects are quite common. There are indications that sodium might be an important element for these objects. Motivated by these astronomical observations, the aim of the present work is to study the atomic structure of the sodium atom in a weak to intermediately strong magnetic field.

Many-electron systems in a magnetic field behave in a complicated way. Reasons for this are the competing magnetic, electron-nucleus and electron-electron interactions. Different electrons possess different one-particle energies, which means that the intermediate field regime of the atom becomes the sum of the intermediate fields regimes for the different electrons. The number of investigations on systems with more than two electrons is very scarce [18–25]. Several of these works [18–21] have studied exclusively the high field regime by means of the adiabatic approximation. Clearly the corresponding methods can not be used to describe the behaviour of these systems in the intermediate field regime, which is the most important in terms of astronomical observations. The ground state and a few excited states of the atoms H to Ne, as well as their positive ions in strong magnetic fields have been investigated using a two-dimensional mesh Hartree-Fock method [22–25]. In reference [26] strong magnetic fields have been used to influence the generation of higher harmonics for the H^- and Ar atoms in a linearly polarized laser field. The mechanism of charge-resonance-enhanced ionisation for the H_2^+ molecule in a strong magnetic field parallel to a laser field was studied by means of a highly accurate numerical procedure in reference [27].

Currently there exists no implemented general method to perform *ab initio* studies of the properties of arbitrary many electron atoms ($N > 2$) in a magnetic field. To describe these systems it is therefore adequate to develop alternative approaches. A promising one are the model potentials that have been successfully applied in different areas of atomic physics. The key idea is the following. The atom is divided into two parts: a valence part (open shell) and a closed shell multielectron core including the nucleus. The core is then replace by a suitably chosen model potential which, when it is introduced into the Hamiltonian, reproduces as close as possible the true spectrum of the interacting system. The initial multielectron problem is thereby reduced to an effective one-particle problem. Of course one has to take care of the validity of the model potential approach which is limited to those parts of the spectrum where it is sufficient to exclusively consider excitations of the valence electron. Excitations of the closed shell core correspond to much higher energies and can therefore be safely neglected. In particular, a model potential for the alkali atoms and the Li isoelectronic sequence is presented in reference [28]. In this reference binding energies, effective quantum numbers and oscillator strengths for various transitions have been computed, and compared with experimental data as well as other theoretical studies.

Due to the atomic structure of the sodium atom ($1s^2 2s^2 2p^6 3s$), *i.e.* a single valence electron in a $3s$ orbital, one can assume that for a certain regimen of field strengths the magnetic field only affects the external electron. We can therefore work in the frame of a "single active electron" approximation assuming that the core electrons are frozen in their initial orbitals, *i.e.* not affected by the external field. This approximation is valid for low to moderate field strengths. Due to the large energetical gap of the excitation of the core for the sodium atom we expect that for field strengths $B \lesssim 0.1$ a.u. (the magnetic field is measured in atomic units $B_0 = 2\alpha^2 m_e^2 c^2/\hbar e \approx 4.701 \times 10^5$ T) field effects on the core can be neglected.

With the help of the model potential presented in [28] we study the spectrum of the sodium atom in a magnetic field of intensity $B = 0.0-0.02$ a.u. assuming that the electron-core interaction is unaltered by the external magnetic field. The ionisation energies and dipole transitions of all states with principal quantum numbers $n = 3-7$ including all angular symmetries are investigated with increasing field strength. Dipole strengths, oscillator strengths and the transition rates have been computed. We remark that, to our knowledge, the present work is the first which deals with the sodium atom exposed to a strong magnetic field.

The paper is organised as follows. In Section 2 we define our model potential and we briefly discuss some specifics of our computational method. Section 3 contains the results and the corresponding discussion, including a selection of the obtained ionisation energies, transition wavelengths and oscillator strengths. The conclusions and

outlook are provided in Section 4. Atomic units will be used throughout unless stated otherwise.

2 Hamiltonian, computational method and techniques

The aim of the model potential is to mimic the interaction of the valence electron with the multielectron core by means of an effective potential, which is an analytic continuation of the Coulomb potential. The model potential used in [28] to describe the valence electron of an alkali atom or an alkali like ion has the following form:

$$V(r) = -\frac{1}{r}\left(\tilde{Z} + (Z-\tilde{Z})\mathrm{e}^{-a_1 r} + a_2 r \mathrm{e}^{-a_3 r}\right), \quad (1)$$

where Z is the atomic number, $\tilde{Z}$ is the ionisation stage (it is 1 for neutral atoms, 2 for singly ionisated atoms and so forth), a_1, a_2 and a_3 are the model potential parameters. This model potential satisfies the appropriate boundary condition and has the advantage of having no additional higher order singularities than the Coulomb term. For the case of sodium, $Z = 11$ and $\tilde{Z} = 1$, the optimised values of these parameters [28] are given by:

$$a_1 = 7.902, \quad a_2 = 23.510, \quad a_3 = 2.688.$$

The optimisation of these parameters was done in the field-free case without referring to any special energy range, because in the presence of an external field the principal quantum number is no more valid, and states with the same symmetry in the presence of the magnetic field will mix.

We adopt a nonrelativistic frame: for the field strengths considered here the relativistic corrections are smaller than the accuracy of our results. The Hamiltonian of our effective one-particle atomic system, assuming an infinitely heavy core, reads as follows:

$$H(r,\vartheta,\varphi) = -\frac{1}{2r^2}\frac{\partial}{\partial r}r^2\frac{\partial}{\partial r} + \frac{1}{2r^2}L^2(\vartheta,\varphi) - \mathrm{i}B\frac{\partial}{\partial\varphi} + \frac{B^2}{2}r^2\sin^2\vartheta + V(r), \quad (2)$$

where the uniform magnetic field points along the z-axis. This Hamiltonian commutes with the z-component of the orbital angular momentum l_z and the z-parity operator Π_z. The corresponding quantum numbers m and π_z will be used to label the atomic states. In the absence of the field ($B = 0$) we have the full rotational symmetry and the above Hamiltonian is integrable. The corresponding quantum states can be labelled by the quantum numbers n, l and m.

The computational method used to solve the one-particle effective Schrödinger equation is based on a combination of a discrete variable technique, applied to the angular coordinates, and a finite element method, applied to the radial variable. These methods result in a generalised eigenvalue problem, which is solved with the help of a Krylov type approach. It has been shown that this computational technique is an accurate and efficient tool to describe nonintegrable quantum systems [29]. A further advantage of this method is the flexibility to include in a simple manner additional potentials, such us magnetic, electric or van der Waals interactions. Thus by including model potentials we can investigate accurate spectra for alkali metal atoms and alkali-like ions. For a detailed description of our computational method we refer the reader to reference [29].

3 Results and discussion

Using the techniques discussed in Section 2 we solve the Schrödinger equation belonging to the effective Hamiltonian (2) in order to obtain the transition energies and their oscillator strengths as well as the ionisation energies of the sodium atom. We cover the regime $B = 0.0{-}0.02$ a.u., taking a grid of twenty different field strengths. This range of field strengths covers the low to intermediate field regime which is of particular relevance to astronomical observations. In the following the quantum numbers n, l and m of the states without field will frequently be used to refer to the states in the presence of the field. Although this procedure facilitates both the assignment of quantum states with and without field and their evolution into each other, it should not obscure the fact that only good quantum numbers in the presence of the field are the magnetic quantum number m and the z-parity π_z. However, mixing of states with different principal quantum number n becomes relevant only for higher excitations and/or stronger fields.

We have studied all states emerging from field-free states with principal quantum numbers $n = 3{-}7$, *i.e.* for any allowed value for the orbital and magnetic quantum numbers $l \leq n-1$, $|m| \leq l$. All allowed electric dipole transitions between these states have been computed, *i.e.* transition wavelengths, dipole strengths, oscillator strengths and transition rates. Due to the large amount of data we can provide here only a graphical illustration of the behaviour and properties of the above quantities with changing field strength. Tables with numerical values to be used and applied by astronomers will be presented elsewhere.

3.1 Ionisation energies

In this section we illustrate our results on the ionisation energies as a function of the field strength for the states which emerge from field-free states with principal quantum numbers $n = 3{-}7$, $l \leq n-1$ and $m = 0, -1$ and -2, including positive and negative z-parity. Due to the symmetries of the Hamiltonian, the energies of the states with $m > 0$ are obtained by a simple shift from those of the states with $m < 0$. Hence, we show here exclusively the energies for states with $m < 0$.

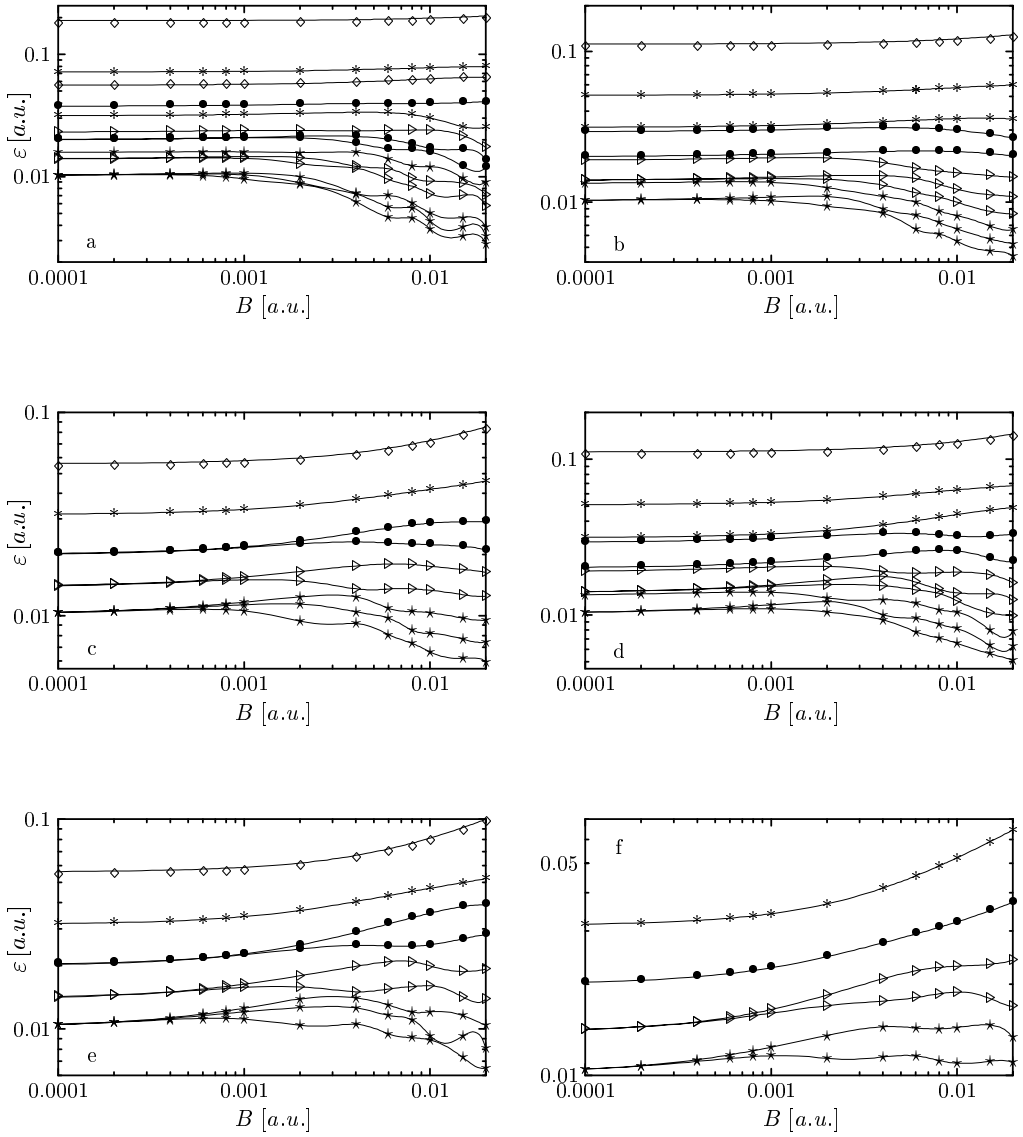

Fig. 1. The one-particle ionisation energies for states emerging from field-free states with principal quantum number $n = 3{-}7$ as a function of the magnetic field strength. The symbols ($\diamond$, $*$, $\bullet$, $\triangleright$, $\star$) were taken for states with $n = 3{-}7$, respectively. In (a) and (b) we show the ionisation energies for states with $m = 0$ positive and negative z-parity, respectively. Figures (c) and (d) show the ionisation energies for states with $m = -1$ positive and negative z-parity, respectively. Corresponding Figures (e) and (f) show the ionisation energies for states with $m = -2$ positive and negative z-parity, respectively.

3.1.1 Results for m = 0 positive and negative z-parity

The one-electron ionisation energies refer to the process $\mathrm{Na} \rightarrow \mathrm{Na}^+ + e^-$. The one-particle ionisation threshold is given by the lowest possible total energy for which the system $\mathrm{Na}^+ + e^-$ exists, *i.e.* it is given by the sum of the ground Landau level of the free electron in the field plus the energy of the remaining multielectronic core, Na^+. We mention that for specific ionisation processes (electromagnetic transitions) the threshold might be different from the above-defined one due to the conservation of certain symmetries, *i.e.* quantum numbers, in the course of the ionisation process. The remaining core, Na^+, is in our case assumed not to be significantly affected by the magnetic field. Hence, we obtain the following one-particle ionisation energy

$$\varepsilon = B - E, \tag{3}$$

where E is an eigenvalue of the Hamiltonian (2). Within our computations we have followed the convergence criterion of six converged digits for the energies with $n \leq 6$ and four converged digits for $n = 7$. We would like to remark that the states with $m = 0$ were the most difficult to obtain within the above accuracy, *i.e.* we had to use a particularly large number of functions and grid points within the discrete variable technique.

In Figure 1a we illustrate the one-particle ionisation energies for the states with $m = 0$ and positive z-parity as a function of the magnetic field strength. Logarithmic

scales are used for the ionisation energies and the magnetic field strength to cover the several orders of magnitude. The ionisation energy of the ground state of the system (uppermost curve in Fig. 1a) monotonically increases as the field is increased, *i.e.* the ground state becomes more strongly bound. Within the regime of field strengths considered here ($B = 0.0-0.02$ a.u.) the increase amounts to 0.017 a.u. The first three excited states show a similar behaviour, *i.e.* they are weakly affected by the magnetic field and become increasingly bound with increasing field strength. This is not true for the higher excited states. For low field strengths $B \lesssim 10^{-3}$ a.u. their ionisation energies gradually increase whereas for higher field strengths they first decrease and then show an oscillatory dependence on the field strength. As expected the onset of this behaviour depends on the degree of excitation, *i.e.* it occurs for higher excited states at lower field strengths. This demonstrates the well-known fact that the so-called strong field regime depends on the degree of excitation. In the field-free sodium atom the quantum defect for states with a large value for the orbital quantum number $l \geq 2$ is close to zero, the energies for the valence electron are very similar and the states become quasi degenerate. In Figure 1a we observe how this degeneracy is lifted with increasing field strength. It is particularly evident for those states with principal quantum number $n = 5$, 6 and 7. This phenomenon will also be present for the other states with different values of the magnetic quantum number and z-parity (see following figures).

At $B \sim 0.002$ a.u. two states with $n = 7$ exhibit an avoided crossing, the same effect appears again around $B \sim 0.004$ a.u. for two states with $n = 7$ and for two states with $n = 6$, and also at $B \sim 0.01$ a.u. for two states with $n = 5$. This is due to the fact that the states shown in Figure 1a, that are different by symmetry for $B = 0$, possess the same symmetry for $B \neq 0$ and are therefore not allowed to cross.

In Figure 1b we show the one-particle ionisation energy for the states with $m = 0$ and negative z-parity as a function of the field strength. They show a similar behaviour to the one shown for the positive z-parity states in Figure 1a. However, for higher excited states and strong fields the oscillatory behaviour of the ionisation energies for the negative z-parity states is much less pronounced compared to the positive z-parity states discussed above, *i.e.* we encounter less narrow avoided crossings and almost parallel ionisation curves. For stronger fields 0.02 a.u. $> B >$ 0.002 a.u. the overall tendency of the ionisation energy of the states with $m = 0$ is a decrease with increasing field strength.

3.1.2 Results for m = −1 and m = −2 positive and negative z-parity

In Figure 1c we show the one-particle ionisation energy for states with $m = -1$ and positive z-parity as a function of the magnetic field strength, and in Figure 1d the corresponding results for states with $m = -1$ and negative z-parity. The three energetically lowest states with positive z-parity and the first two for negative z-parity show a weak monotonous increase of their ionisation energies as the field strength increases. Many of the statement given above for the $m = 0$ states hold also here, although the detailed individual quantitative behaviour of the energy curves is of course different.

The ionisation energies of the states with $m = -2$ and positive and negative z-parity are shown in Figures 1e and 1f, respectively. First we observe that the low-lying states show a stronger increase of their ionisation energies with increasing field strength for states with $m = -1$ compared to those with $m = 0$ and analogously for those with $m = -2$ compared to those with $m = -1$. Generically the relative increase of the ionisation energies for the negative z-parity states is always smaller than that of the positive z-parity states. For $B > 0.001$ a.u. we now observe an envelope behaviour of the ionisation energy curves of the higher excited states which is remarkably different from the corresponding $m = 0$ curves: for the $m = -1$ states it is a weak decrease and for the $m = -2$ states an approximate constant.

3.1.3 Comparison with the hydrogen atom

The fact that the sodium atom possesses a single electron in the $3s-$shell and a closed shell core otherwise allows for our single active electron approach. It is therefore natural to perform a comparison of the sodium spectrum with the spectrum of the hydrogen atom in particular in the presence of a magnetic field. To this end we have calculated the corresponding energy eigenvalues of the hydrogen atom.

Figure 2a shows the one particle ionisation energies for the states with $m = 0$ and principal quantum number $n = 3-6$ as a function of the magnetic field strength for the sodium atom and Figure 2b illustrates the corresponding energies for the hydrogen atom. The two spectra show important differences. First one should note the well-known splitting of the energies belonging to states with different orbital angular momentum in case of the sodium atom compared to the degeneracies for the hydrogen atom (for $B = 0.0001$ in Fig. 2 these are, of course, near degeneracies). Also the ranges of the ionisation energies are different for the two spectra: for the sodium atom the states with principal quantum number $n = 3, 4$ are more strongly bound than for the hydrogen atom. Although Figure 2 clearly shows the different evolution of the hydrogen and sodium spectra with increasing field strength lets briefly discuss one example for this evolution in more detail. For the hydrogen atom (Fig. 2b) the ionisation energies of the $3d_0$ and $3p_0$ states monotonically increase with increasing magnetic field strength, while the ionisation energy of the state $3s$ first increases up to a certain value of the field strength and thereafter decreases. Within the regime of field strength consider here the increase in the ionisation energy of the $3d_0$ state amounts to 0.0099 a.u., and the decrease of the energy for the state $3s$ amounts to 0.0023 a.u. For the sodium atom the behaviour of the $3s$-state is opposite *i.e.* this state is much more affected by the external

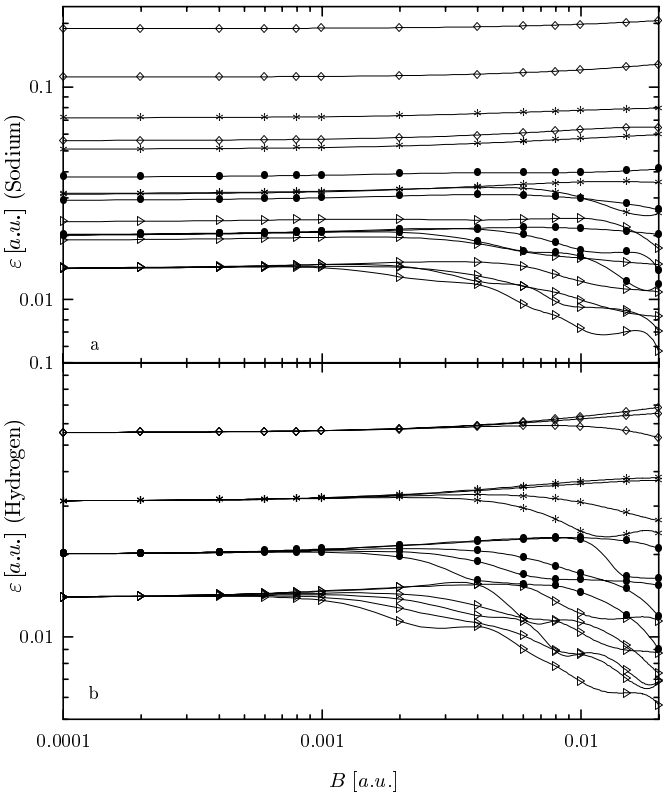

Fig. 2. The one-particle ionisation energies for states emerging from field-free states with principal quantum number $n = 3{-}6$ as a function of the magnetic field strength. The symbols ($\diamond$, $*$, $\bullet$, $\triangleright$) were taken for states with $n = 3{-}6$, respectively. In (a) we show the ionisation energies for the sodium atom, (b) shows the corresponding results for the hydrogen atom.

field and becomes stronger bound. From the above it is evident that the spectral properties of the sodium atom in a magnetic field even qualitatively cannot be derived from those of the hydrogen atom in the corresponding field.

3.2 Transition wavelengths

The central motivation to study the atomic spectrum of sodium in a magnetic field is to advance the interpretation of observed absorption spectra of a new kind of magnetic white dwarf stars. Some of these objects with very weak fields show already strong evidence for the presence of heavy atoms such as Na, Ca or Mg [17]. Key quantities are therefore the wavelengths of the transitions between low-lying excited states. A broad regime of field strengths has to be covered since the field strength can vary significantly from object to object, and second because the magnetic field in the atmosphere of a star is not constant, but typically varies by a factor of two for a dipole geometry. Indeed, it is necessary to analyse a large amount of transitions. For somewhat strong fields one has to search for those lines which develop a stationary behaviour as a function of the magnetic field: only stationarily lines leave their fingerprints and are not smeared out in the observed spectra. For weak fields and/or lines which depend only very weakly on the field strength the stationarity argument is relaxed.

We study in the following electromagnetic dipole transitions. In the presence of the magnetic field the allowed transitions are given by the selection rules $\Delta m = m_\mathrm{i} - m_\mathrm{f} = 0, \pm 1$ and a change in z-parity between the initial and final state, being m_i and m_f their respective magnetic quantum numbers. They can be classified as circular polarised transitions for $\Delta m = \pm 1$, and as linear polarised for $\Delta m = 0$. Due to the large amount of data obtained we restrict ourselves to a graphical presentation of the transitions with initial states that possess in the field-free case an orbital angular quantum number $l = s, p, d$. The initial magnetic quantum number then varies as $m = 0, \pm 1 \pm 2$ and the final one is restricted to $m = 0, \pm 1 \pm 2, \pm 3$. For the states considered here ($n = 3{-}7$) there are 16 circular polarised transitions, *i.e.* there are 16 different combinations of the pair of quantum numbers for the initial $(m_\mathrm{i}, \pi_{z_\mathrm{i}})$ and final states $(m_\mathrm{f}, \pi_{z_\mathrm{f}})$, and 8 linear polarised transitions. These results were interpolated and we present them in Figures 3a–3e. Logarithmic scales for the wavelength and for the field strength are used to cover several orders of magnitude, respectively. The range of wavelength was chosen such that it contains in particular the astronomically relevant regime (see Figs. 3a–3e). The chosen range for the field strength is 0.0001 a.u. $\leq B \leq$ 0.02 a.u., for which the transition wavelengths show interesting properties.

Figures 3a–3e show the transition wavelengths as a function of the field strength for all the transitions with the initial (field-free) states $\{ns, nd, nd\}$ for $n = 3{-}7$ to the final states with $n' = n{-}7$, respectively. (We remind the reader of the fact that both n and l are not good quantum numbers in the presence of the field but are just used as a label to make the unique assignment with the corresponding field-free states.) These figures demonstrate the large amount of computations that have been accomplished in the present work.

Obviously the overall evolution of the spectrum with increasing field strength is very complex. For $B = 0$ the spectral lines are well-organised in groups, which are characterised by their principal quantum numbers and orbital angular quantum numbers of the corresponding initial and final states. As the magnetic field increases, these groups split into several spectral branches. In particular, one can see here how the approximate degeneracy with respect to the orbital angular quantum number of the states with $l \geq 2$ and the exact degeneracy with respect to the magnetic quantum number are lifted with increasing field strength. The splitting for small values of B of the spectral lines is determined by the value Δm of the transitions. The spectral lines are divided into three groups, characterised by their different values of Δm. In case that for the initial or final state the approximate l-degeneracy occurs, the increasing field strength will yield an additional splitting of the lines. At the same time the m-degeneracy is also lifted and each line shows a different evolution with changing field strength.

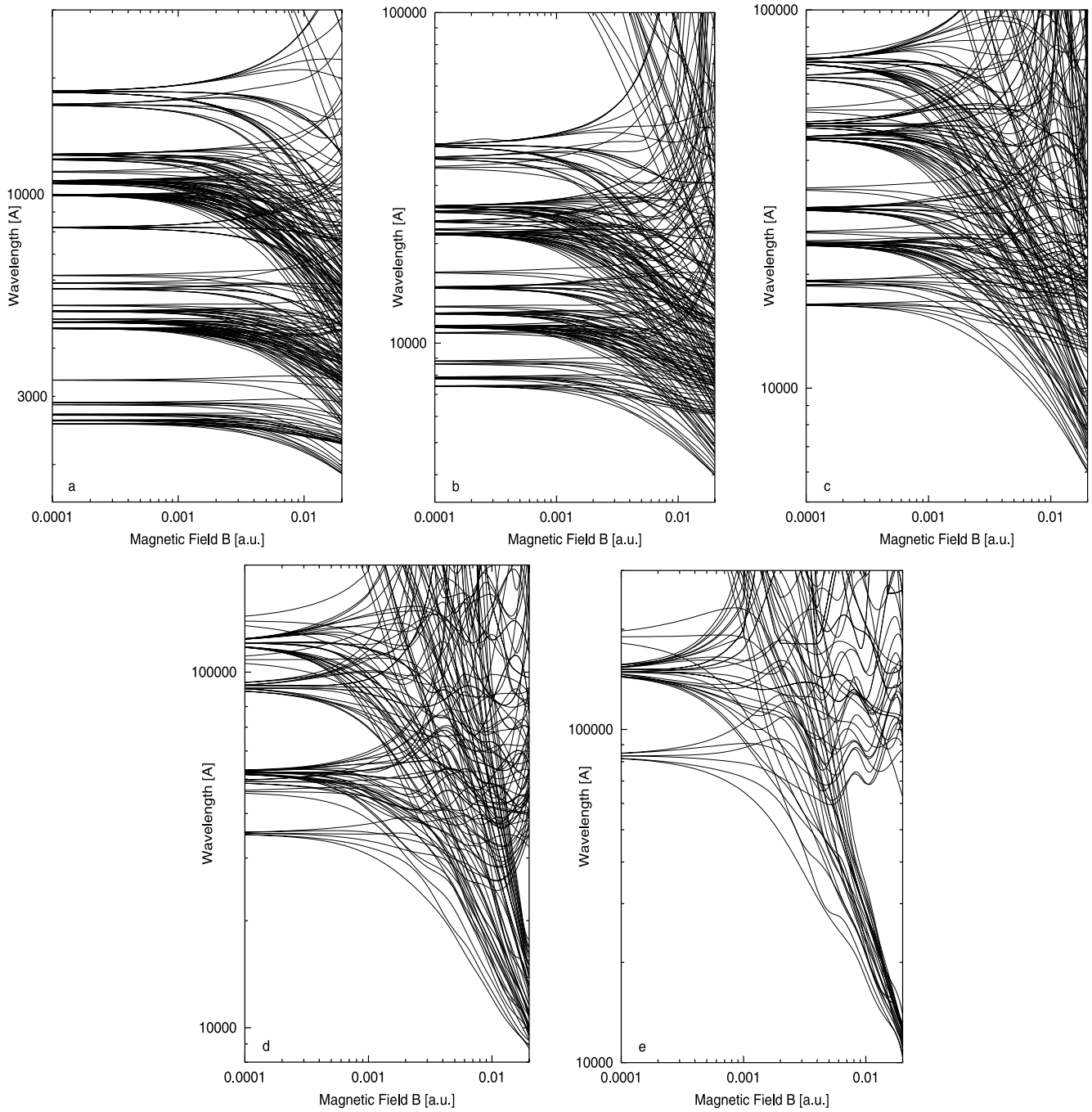

Fig. 3. The wavelengths of the electric dipole transitions emerging from field-free states with principal quantum numbers $n = 3{-}7$ and orbital angular quantum number $l = 0, 1, 2$ and the corresponding final states $n' = n - 7$, as a function of the magnetic field strength. Figures (a–e) show the results for the transitions with initial states $n = 3{-}7$, respectively.

The behaviour of the spectral lines becomes more complicated as the principal quantum number of the initial state involved increases. For those transition emanating from the states $3s, p, d$ the wavelengths as a function of the magnetic field show in most of the cases a smooth behaviour (see Fig. 3a). Some of the spectral lines are affected very weakly by the field, and they appear as almost horizontal lines in our graphical representation of the spectra. There are only a few lines possessing a more interesting evolution: their wavelengths change significantly as the field increases, or they even show a stationarity for a certain value of the field strength. For the transitions with initial states $4s, p, d$ (see Fig. 3b) there are still some spectral lines being weakly affected by the external field. However the number of transitions with an irregular behaviour has increased. Comparing Figures 3b and 3a we observe that the splitting of the spectral lines occurs for lower field strengths, and the regime of strong

mixing is enlarged. These tendencies are even more pronounced for the higher initial excitations: Figures 3c–3e correspond to the initial states $nspd$, $n = 5-7$ respectively. For $n = 7$ in Figure 3e our choice for the field strength regime 10^{-4} a.u. $\leq B \leq 0.02$ a.u. contains no spectral curves which are very weakly dependent on the field strength, *i.e.* the splitting is already significant for $B = 10^{-4}$ a.u. The irregular behaviour is also more pronounced for these higher values of the principal quantum number of the initial state. The $n = 5-7$ spectra (Figs. 3c–3e) exhibit a significant number of spectral lines that become stationary for some critical field strength.

We remark that level crossings of the initial and final states yield stationary lines for divergent wavelengths, that are, due to the chosen range of wavelengths, not included in our figures.

3.3 Oscillator strengths

The wavelengths of the dipole transitions are not sufficient to perform a *detailed* analysis of the observed astronomical spectra. Indeed, to provide synthetic spectra by simulations of the radiation transport in the atmosphere of the white dwarf star, the oscillator strengths of the transitions have to be known. (We consider here only bound-bound transitions although bound-free and even free-free transitions contribute also to the appearance of the synthetic spectra). For each bound-bound transition considered here we have computed the dipole strength, the oscillator strength and the transition rate. These three quantities provide different measures for the probability of a transition. In this section we present selected results for the oscillator strengths of the dipole transitions.

A common way of expressing the strength of a transition is via the oscillator strength, which we have computed in the length form. Working in first order perturbation theory for the electromagnetic transition, using the dipole approximation by assuming that the wavelengths of the transitions are larger than the typical size of the atom, the expression in atomic units for the oscillator strength $f^{(q)}_{\alpha\beta}$ of a dipole transition is given by:

$$f^{(q)}_{\alpha\beta} = 2(E_\beta - E_\alpha) d^{(q)}_{\alpha\beta} \quad \text{with} \quad d^{(q)}_{\alpha\beta} = \left| \langle \psi_\alpha | r^{(q)} | \psi_\beta \rangle \right|^2 \quad (4)$$

where $d^{(q)}_{\alpha\beta}$ is the dipole strength of the spectral line, $r^{(q)} = \sqrt{4\pi/3}\, r Y_{1q}$ are the spherical components of the dipole operator, α and β denote the set of quantum numbers characterising the initial and final states, respectively, E_α and E_β are their corresponding energies, ψ_α and ψ_β their corresponding wavefunctions.

Due to the large amount of data obtained in the present investigation, we are not able to provide them numerically and even a graphical presentation has to confine itself to a selected subset of data. In the following we show examples of how the oscillator strengths and the wavelengths change with the magnetic field strength: for a selected group of transitions we have chosen five values for the magnetic field strength $B = 0.0$, 0.0002, 0.002, 0.008 and 0.02 a.u. The values $f(\lambda; B)$ for different field strengths have been included in the same figure to facilitate their comparison, obtaining in this way a nice global view of the evolution of the spectrum, *i.e.* the transition wavelengths and their oscillator strengths.

Figures 4a and 4b describe circular and linear polarised transitions emanating from the $n = 3$-manifold to a final state with $n = 3-7$, respectively. Figures 4c and 4d show the results on circular and linear polarised transitions with and initial state belonging to $nl = 4s$, $4p$, $4d$ and a final state possessing a principal quantum number in the range $4-7$, respectively. For the circular polarised transitions only transitions involving states with $m \leq 0$ have been taken into account.

Before starting with a detailed description of our data in the presence of the field, it is interesting to point out the physics in the field-free case and analyse the corresponding transitions. The corresponding results are given in the first row of Figures 4a–4d. In the field-free case, the states are characterised by the principal, orbital angular and magnetic quantum numbers, nl and m respectively. The selection rules for the dipole transitions are $\Delta l = \pm 1$ and $\Delta m = \pm 1$ for circular polarised and $\Delta m = 0$ for linear polarised transitions. Due to these selection rules the number of allowed transitions is comparatively small. The energy eigenvalues of the atom are degenerate with respect to the magnetic quantum number m. Consequently the dipole transition energies and rates between two states with quantum numbers nl and $n'l'$ are independent of their magnetic quantum numbers. In particular there is no difference between linear polarised and circular polarised transitions among these manifolds, as one can see by comparison of the first rows of Figures 4a and 4b for the transitions starting with $n = 3$, and correspondingly the first rows of Figures 4c and 4d for initial states $n = 4$.

Let us now concentrate on the analysis of Figure 4a. For the first non-zero field strength ($B = 0.0002$ a.u.), which is still a quite weak magnetic field, the spectral lines, which were already present in the field free spectrum, have not changed significantly: they are approximately at the same positions and have approximately the same oscillator strengths. The most interesting effect is the appearance of new spectral lines that correspond to transitions that were forbidden for $B = 0$. They emerge from the splitting of the field-free spectral lines because the presence of the magnetic field destroys the m-degeneracy. The wavelengths of the new transitions is close to the wavelengths of the allowed transitions for $B = 0$. In some cases they can hardly be recognised in Figures 4a–4d. Of course, the corresponding oscillator strengths acquire a finite value exclusively due to the presence of the field. The effect of the magnetic field is more pronounced for the values $B = 0.002$, 0.008, 0.02 a.u. of the field strength. The number of allowed transitions has increased drastically. In general, the wavelengths of the transitions are shifted to smaller values, and new transitions appear whose wavelengths were beyond the regime represented in the figures

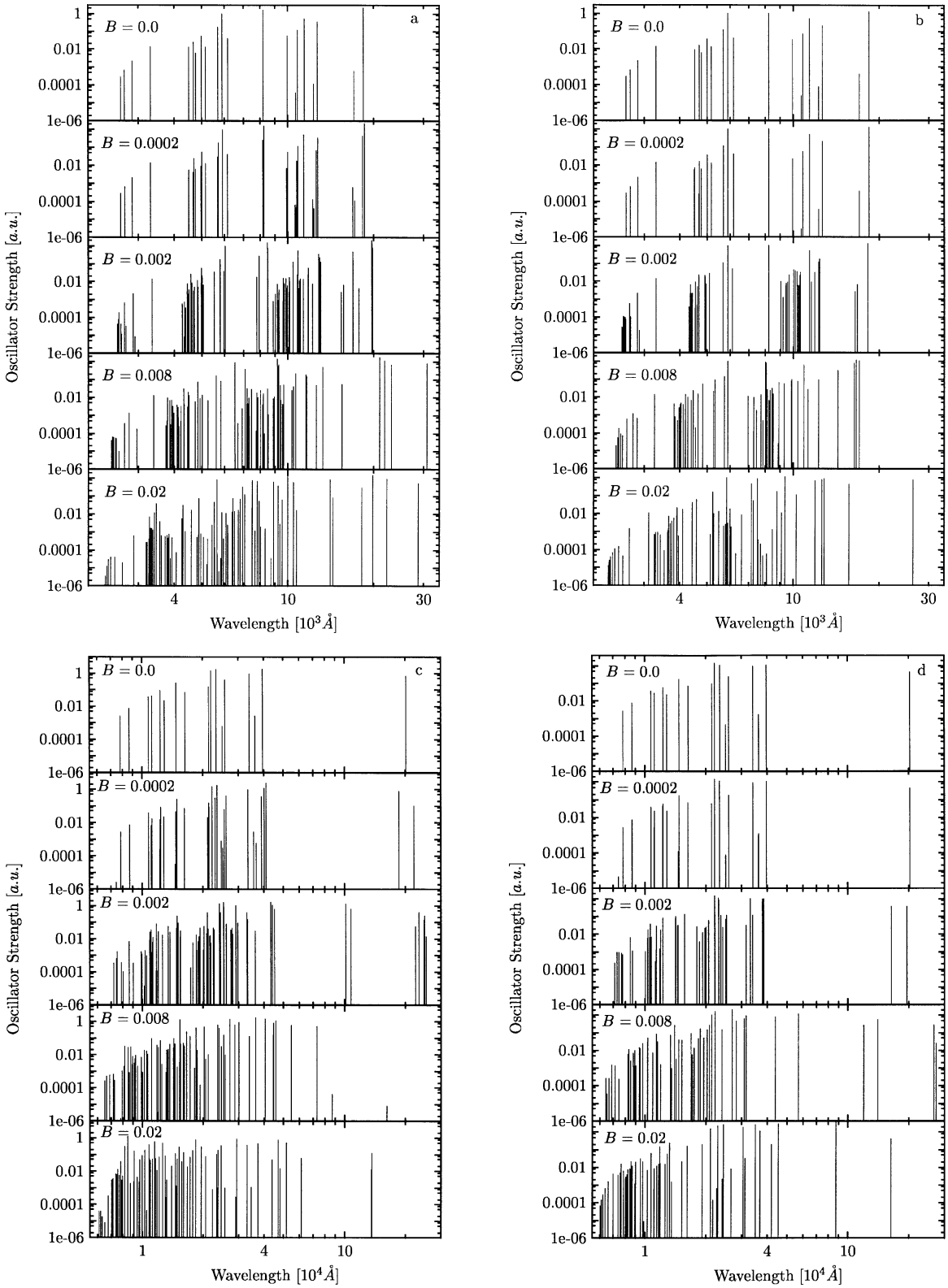

Fig. 4. The oscillator strengths for certain dipole transitions as a function of their wavelengths for five different field strengths $B = 0.0$, 0.0002, 0.002, 0.008 and 0.02 a.u. from top to the bottom. Figures (a) and (b) show the results for those transitions emanating from the states with principal quantum number $n = 3$ and having final states $n = 3-7$, for circular and linear polarisation, respectively. Figures (c) and (d) show the results for the transitions emanating from the states with quantum number $\{4s, 4p, 4d\}$ and final states with $n = 4-7$ for circular and linear polarisation, respectively.

for lower field strengths. For $B = 0.002$ and 0.008 a.u., two major groups of transitions can still be identified in the figures, each one of them originating from the corresponding group of the $B = 0$-spectrum. For the largest field strength $B = 0.02$ a.u. the groups of spectral lines are completely mixed up. Needless to say that the oscillator strengths of the transitions also change a lot: some transitions are favoured, and others will become less probable or extremely small. In particular, for $B = 0.0$, 0.0002, 0.002, 0.008 a.u., there is an isolated transition with wavelength $\lambda \sim 3300$ Å which is almost independent on the field strength: it is shifted very little with increasing field strength. For $B = 0.02$ a.u. it is hidden in a group of transitions with similar wavelengths and its wavelength has decreased significantly. Also, with increasing field strength its oscillator strength decreases weakly. This transition is $3s \rightarrow 4p_{-1}$, and the observed smooth behaviour with the magnetic field is related to the smooth behaviour of the total energies of these two states with the field (see Sect. 3.1 for ionisation energies). A similar evolution holds for the wavelength and oscillator strength of the $3s \rightarrow 3p_{-1}$ transition, however it is not so isolated in the spectrum but hidden in a large number of spectral lines.

Figure 4b shows characteristics of the linear polarised transitions with the initial state $n = 3$. Many features discussed above can also be observed here. Of course, there are fewer transitions compared to the circular polarisated ones in Figure 4a. Again there is an isolated transition at $\lambda \sim 3300$ Å that is $3s \rightarrow 4p_0$. Its wavelength and oscillator strength are weakly affected by the field, and for $B = 0.02$ a.u. it is modified most. A further isolated spectral line belonging to the transition $3s \rightarrow 3p_0$ for $B = 0.0$, 0.0002, 0.002, 0.008 a.u. occurs at $\lambda \sim 8000$ Å, possessing a smooth and weak dependence on the field.

For the transitions with initial states $n = 4$, one observes in Figures 4c and 4d that the spectrum becomes tentatively more complicated compared to the transitions emanating from $n = 3$. The main difference is a global shift to the infrared. Again, in these two spectrum there are new spectral lines that appear for higher values of the magnetic field on the long wavelength part of the spectrum. The transitions $4s \rightarrow 4p_0$, $4s \rightarrow 4p_{-1}$, $4d_m \rightarrow 4p_m$, $4d_m \rightarrow 4p_{m\pm1}$, show a rather smooth evolution with the magnetic field, however they cannot be easily identified in the spectrum.

4 Brief conclusions and outlook

We have investigated the electronic structure of the sodium atom in a magnetic field by describing the system with the help of a model potential in an effective one-electron approach. We assume that the external field only affects the valence electron significantly, and the core electrons are frozen in their field-free configuration. We have also applied the infinitely heavy nucleus approximation. The Schödinger equation of the valence electron was solved by a computational method based on a combination of a discrete variable representation and a finite element method.

We covered the astronomically important field regime 0.0 a.u. $\leq B \leq$ 0.02 a.u., *i.e.* the weak to intermediate region, depending on the degree of excitation. We investigated twenty values for the field strength, and computed the energies of all states with principal quantum number $n = 3{-}7$, *i.e.* in total 20×135 states and 20×1584 dipole transitions. In principle our approach holds still for somewhat larger field strengths. However the computational effort to investigate *e.g.* the regime 0.02 a.u. $< B <$ 1.0 a.u. is enormous. The present investigation amounted already to a total of 5 months of CPU on a work station with 1 GHz Pentium III processor. A full account of the ionisation energies, the transition wavelengths and their oscillator strengths (electric dipole transitions) among all states $n = 3{-}7$ with varying magnetic field has been given. Due to the large amount of obtained results and data we provide here only a selection of them, by use of graphical presentations. Examples for the breaking of the degeneracies of the system, have been nicely observed by the splitting of the spectral lines with increasing field strength.

We expect that the present results should be of major help towards the interpretation of the spectra of the new type of magnetic white dwarfs, that are believed to contain heavier elements such as Na in their atmospheres. The present results can also be used to confirm the first interpretation given in reference [17] for the absorption features of the LH 2534 white dwarf star in terms of the sodium atom.

As already indicated above an immediate extension of the present work would be to extend the computations to stronger field and states with higher principal quantum number $n > 7$.

R.G.F. gratefully acknowledges a scholarship by the Alexander von Humboldt Foundation and financial support for traveling by the Spanish project BFM2001-3878-C02-01 (MCYT). We thank J. Liebert for drawing our attention to the relevance of sodium in a strong magnetic field to astronomical observations. We thank I. Lesanovsky for providing us with the results on the hydrogen atom in a magnetic field.

References

1. H. Friedrich, D. Wintgen, Phys. Rep. **183**, 37 (1989)
2. G. Wunner, H. Ruder, H. Herold, Astrophys. J. **247**, 374 (1981)
3. H. Forster, W. Strupat, W. Rösner, G. Wunner, H. Ruder, H. Herold, J. Phys. B **17**, 1301 (1984)
4. R.J.W. Henry, R.F. O'Connell, Astrophys. J. **282**, L97 (1984)
5. W. Rösner, G. Wunner, H. Herold, H. Ruder, J. Phys. B **17**, 29 (1984)
6. H. Ruder, G. Wunner, H. Herold, F. Geyer, *Atoms in Strong Magnetic Fields* (Springer Verlag A-A, 1994)
7. Yu.P. Kravchenko, M.A. Liberman, B. Johansson, Phys. Rev. A **54**, 287 (1996)
8. *Atoms and Molecules in Strong External Fields*, edited by P. Schmelcher, W. Schweizer (Plenum Press, 1998)
9. D.T. Wickramasinghe, L. Ferrario, Publ. Astron. Soc. Pacific **112**, 873 (2000)

10. W. Becken, P. Schmelcher, F.K. Diakonos, J. Phys. B **32**, 1557 (1999)
11. W. Becken, P. Schmelcher, J. Phys. B **33**, 545 (2000)
12. W. Becken, P. Schmelcher, Phys. Rev. A **63**, 053412 (2001)
13. W. Becken, P. Schmelcher, Phys. Rev. A **65**, 033416 (2002)
14. S. Jordan, P. Schmelcher, W. Becken, W. Schweizer, Astron. Astrophys. Lett. **336**, L33 (1998)
15. S. Jordan, *12th European Workshop on White Dwarfs, ASP Conference Proceedings*, edited by J.L. Provencal, H.L. Shipman, J. MacDonald, S. Goodchild (Astronomical Society of the Pacific, San Francisco, 2001), Vol. 226, p. 269
16. D. Reimers, S. Jordan, V. Beckmann, N. Christlieb, L. Wisotzki, Astron. Astrophys. **337**, L13 (1998)
17. I.N. Reid, J. Liebert, G.D. Schmidt, Astrophys. J. **550**, L61 (2001)
18. E. Müller, Astron. Astrophys. **130**, 415 (1984)
19. D. Neuhauser, S.E. Koonin, K. Langanke, Phys. Rev. A **36**, 4163 (1987)
20. M. Demeur, P.-H. Heenen, M. Godefroid, Phys. Rev. A **49**, 176 (1994)
21. M.D. Jones, G. Ortiz, D.M. Ceperley, Phys. Rev. A **54**, 219 (1996)
22. M.V. Ivanov, P. Schmelcher, Phys. Rev. A. **57**, 3793 (1998)
23. M.V. Ivanov, P. Schmelcher, Phys. Rev. A. **60**, 3558 (1999)
24. M.V. Ivanov, P. Schmelcher, Phys. Rev. A. **61**, 022505 (2000)
25. M.V. Ivanov, P. Schmelcher, J. Phys. B **34**, 2031 (2001)
26. D.B. Milošević, A. Starace, Phys. Rev. A **60**, 3160, (1999)
27. A.D. Bandrauk, H.Z. Lu, Phys. Rev. A **62**, 053406, (2000)
28. W. Schweizer, P. Fassbinder, R. González-Férez, A. Data Nucl. Data Tab. **72**, 33 (1999)
29. W. Schweizer, P. Fassbinder, R. González-Férez, M. Braun, S. Kulla, M. Stehele, J. Comp. App. Math. **109**, 95 (1999)
30. J.C. Light, I.P. Hamilton, J.V. Lill, J. Chem. Phys. **82**, 1400 (1985)